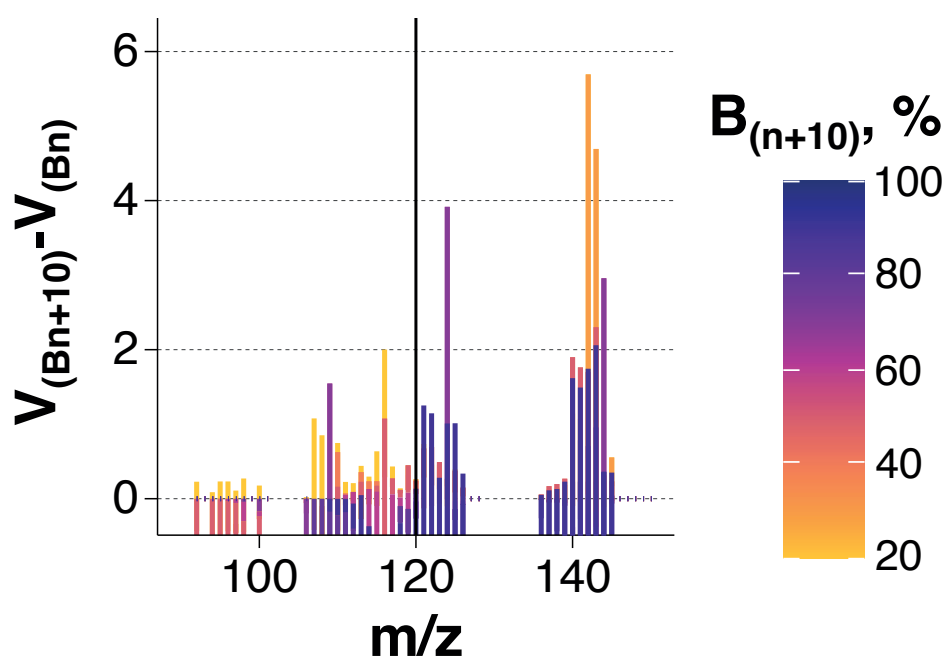


**Supplementary information for:**

**Performance of the double-Wien filter of the Neoma MC-ICPMS/MS with an  
application to copper stable isotope compositions**

Philippe Télouk, Emmanuelle Albalat, Bernard Bourdon, Francis Albarède, Vincent Balter



**Fig. S1:** Difference of overall transmissions from 90 to 150  $m/z$  between two successive masses scans with induction set at  $B(n+10)$  and  $B(n)$ , with  $n$  increasing by 10% increment.

## Ion trajectories in a Wien filter as a function of mass/charge ratio

We assume that the electric and magnetic field are homogeneous and have orthogonal components in the y and x direction, respectively. The z direction corresponds to the main axis of ion trajectories as shown in Figure S1. The ions are injected into the Wien filter with an energy  $E_{kin}$ . The electric and magnetic forces exerted on an ion of charge q and mass m can be written as:

$$q\vec{E} + q\vec{v} \times \vec{B} = m \frac{d\vec{v}}{dt} \quad (1)$$

The electrical field vector has the following components (E, 0, 0) while the magnetic field has the component (0, B, 0). If one uses cartesian coordinates as defined in figure S1, equation (1) is equivalent to the following equation for each coordinate x,y and z:

$$m \frac{dv_x}{dt} = qE - qv_z B \quad (2)$$

$$m \frac{dv_y}{dt} = 0 \quad (3)$$

$$m \frac{dv_z}{dt} = qv_x B \quad (4)$$

We assume that the initial velocity in the direction  $v_y$  is equal to zero and that at  $t=0, y=0$ , thus the second equation is easily integrated to give:

$$y = y_0$$

We thus obtain a system of two coupled second-order equations in the x and z direction:

$$m\dot{v}_x = qE - qv_z B \quad (5)$$

$$\dot{v}_z = \frac{qB}{m} v_x \quad (6)$$

We differentiate equation (6) with respect to time and replace it in equation (5):

$$\dot{v}_x = \frac{m}{qB} \ddot{v}_z \quad (7)$$

$$\frac{m}{qB} \ddot{v}_z = \frac{qE}{m} - \frac{qB}{m} v_z \quad (8)$$

This equation can be rearranged to give:

$$\ddot{v}_z + \left(\frac{qB}{m}\right)^2 v_z = \left(\frac{q}{m}\right)^2 EB \quad (9)$$

It is known from textbooks that the solutions of such equations can first be found by solving the homogeneous equation:

$$\ddot{v}_z + \left(\frac{qB}{m}\right)^2 v_z = 0 \quad (10)$$

A solution to this equation is written as:

$$v_z = A\cos(\omega t) + B\sin(\omega t) \quad (11)$$

With the frequency  $\omega$  equal to:

$$\omega = \frac{qB}{m} \quad (12)$$

We now look for a particular solution to the complete equation. A possible solution could be  $v_z = \text{constant } k$ . In this case:

$$\dot{v}_x = 0 \quad (13)$$

The solution can be written:

$$\left(\frac{qB}{m}\right)^2 k = \left(\frac{q}{m}\right)^2 EB \quad (14)$$

Hence :

$$k = \frac{E}{B} \quad (15)$$

The solution of the complete equation is the sum of the solution of the homogenous equation and the particular solution:

$$v_z = A\cos(\omega t) + B\sin(\omega t) + \frac{E}{B} \quad (16)$$

We now apply the initial condition that  $v_z = v_{init}$  at  $t=0$ . In our system, all the ions are accelerated by a potential of approximately 2 kV to a constant kinetic energy.

$$v_{init} = A + \frac{E}{B} \quad (17)$$

Or :

$$A = v_{init} - \frac{E}{B} \quad (18)$$

In order to determine the value of B, we apply the initial condition for  $v_x$  :

$$\dot{v}_z = -A\omega\sin(\omega t) + B\omega\cos(\omega t) \quad (19)$$

Thus, based on equation (7), we can write:

$$v_x = \frac{m\omega}{qB} [-A\sin(\omega t) + C\cos(\omega t)] \quad (20)$$

The initial condition is that  $v_x = 0$  at  $t=0$ , hence:

$$\frac{m\omega}{qB} C = 0 \quad (21)$$

Thus, we find :

$$v_z = \left( v_{init} - \frac{E}{B} \right) \cos(\omega t) + \frac{E}{B} \quad (22)$$

By integrating with respect to  $t$ , we find the value of  $z(t)$ :

$$z(t) = \frac{1}{\omega} \left( v_{init} - \frac{E}{B} \right) \sin(\omega t) + \frac{E}{B} t + D \quad (23)$$

The constant  $D$  is equal to zero because  $z(t)=0$  at  $t=0$ . The value of  $v_x$  and  $x(t)$  can also be deduced from this:

$$v_x = \frac{m\omega}{qB} \left[ - \left( v_{init} - \frac{E}{B} \right) \sin(\omega t) \right] = - \left( v_{init} - \frac{E}{B} \right) \sin(\omega t) \quad (24)$$

By integrating this equation, we can derive the value of  $x(t)$ :

$$x(t) = \frac{1}{\omega} \left( v_{init} - \frac{E}{B} \right) \cos(\omega t) + K \quad (25)$$

We now apply the initial condition  $x(t)=0$  at  $t=0$ :

$$\frac{1}{\omega} \left( v_{init} - \frac{E}{B} \right) + K = 0 \quad (26)$$

Or :

$$K = - \frac{1}{\omega} \left( v_{init} - \frac{E}{B} \right) \quad (27)$$

The solution for  $x(t)$  is thus:

$$x(t) = \frac{1}{\omega} \left( v_{init} - \frac{E}{B} \right) (\cos(\omega t) - 1) \quad (28)$$

We then use a Taylor expansion of  $\cos(\omega t)$  assuming that  $\omega t$  is small:

$$\cos(\omega t) \approx 1 - \frac{(\omega t)^2}{2} \quad (29)$$

$$x(t) = \frac{1}{\omega} \left( \frac{E}{B} - v_{init} \right) \frac{(\omega t)^2}{2} \quad (30)$$

We also make a Taylor expansion of  $\cos(\omega t)$  in the equation giving  $z(t)$ :

$$\sin(\omega t) \approx \omega t - \frac{\omega t^3}{6}$$

If we choose  $z(t)$  such that it is equal to  $l$ :

$$z(t) = l = \frac{1}{\omega} \left( v_{init} - \frac{E}{B} \right) \omega t + \frac{E}{B} t = v_{init} t$$

We now wish to express  $x(t)$  at the time when the ions exit the Wien filter. To do so, one can use the ions that have an initial velocity equal to  $v_0 = E/B$ . In this case, their velocity  $v_x$  is equal to zero, according to equation ( ) and  $x(t)$  is also equal to zero for these ions. The time  $t$  can be expressed as:

$$t = \frac{l}{v_{init}} \quad (31)$$

This equation can be inserted into equation (30):

$$x(t) = \frac{1}{\omega} \left( \frac{E}{B} - v_{init} \right) \frac{(\omega l / v_{init})^2}{2} \quad (32)$$

$$x(t) = \frac{m}{qB} \left( \frac{E}{B} - v_{init} \right) \left( \frac{qB}{m} \right)^2 \frac{(l/v_{init})^2}{2} = \left( \frac{E}{B} - v_{init} \right) \frac{qB}{m} \frac{(l/v_{init})^2}{2} \quad (33)$$

$$x(t) = (E - v_{init}B) \frac{ql^2}{2mv_{init}^2} \quad (34)$$

The value  $v_{init}$  can be expressed as a function of the initial kinetic energy of the ions  $E_{kin}$  :

$$v_{init} = \sqrt{\frac{2E_{kin}}{m}} \quad (35)$$

This expression is inserted into equation (34):

$$x(z = l) = \left( E - \sqrt{\frac{2E_{kin}}{m}} B \right) \frac{ql^2}{2m_0 v_0^2} \quad (36)$$

We finally obtained the following equation for the deviation in the  $x$  direction of a beam with ions of mass  $m$ :

$$x(z = l) \sim \left( E - \sqrt{\frac{2E_{kin}}{m}} B \right) \frac{ql^2}{4E_{kin}} \quad (37)$$

A more rigorous solution can be obtained by solving for the value of  $t$  the non-linear equation:

$$z(t) = \frac{1}{\omega} \left( v_{init} - \frac{E}{B} \right) \sin(\omega t) + \frac{E}{B} t = l \quad (38)$$

Once the value of  $t$  is obtained, one can calculate the corresponding value of  $x(t)$ . We have checked numerically using a Matlab code that the results are almost identical to those given with the approximate equation (37).

One should point out, however that the deviation calculated with equation (37) does not correspond to the vertical divergence of the beam at the position of the slit. This slit is located a few cm away from the exit of the Wien filter. This means that one also needs to consider the vertical expansion of the beam in the region where no electrostatic or magnetic force is exerted on the ions. In this case, the equations of the trajectory in  $x$  and  $z$  become:

$$m \frac{dv_x}{dt} = 0 \quad (39)$$

$$m \frac{dv_y}{dt} = 0 \quad (40)$$

$$m \frac{dv_z}{dt} = 0 \quad (41)$$

The velocities  $v_x$  and  $v_z$  are constant and the equations can be integrated to yield:

$$x = v_x^0 t + x_0 \quad (42)$$

$$z = v_z^0 t + z_0 \quad (43)$$

We are interested in calculating  $x$  for a given value of  $z=l_2$  representing the distance between the end of the Wien filter and the defining slit. For the sake of simplicity, we take  $x_0$  and  $z_0$  equal to 0. This yields finally:

$$x = \frac{v_x^0}{v_z^0} l_2 \quad (44)$$

This represent a deviation  $\Delta x$  that can be calculated as a function of  $l_2$  and the velocities in  $x$  and  $z$  directions at the exit of the Wien filter:

$$\Delta x = l_2 \frac{\left( \frac{E}{B} - v_{init} \right) \sin\left( \frac{\omega l}{v_{init}} \right)}{\frac{E}{B} + \left( v_{init} - \frac{E}{B} \right) \cos\left( \frac{\omega l}{v_{init}} \right)} \quad (45)$$

This equation must be solved numerically by assuming a value for  $\Delta x$  and one can then obtain the value of  $v_{init}$  corresponding to this vertical deviation. This initial velocity is then converted to the mass of the ion using:

$$m = \frac{2E_{kin}}{v_{init}^2} \quad (46)$$

The total deviation in the x direction is obtained by summing  $\Delta x$  in equation (45) and equation (37):

$$\Delta x_{tot} = \left( E - \sqrt{\frac{2E_{kin}}{m}} B \right) \frac{ql^2}{4E_{kin}} + l_2 \frac{\left( \frac{E}{B} - v_{init} \right) \sin\left( \frac{\omega l}{v_{init}} \right)}{\frac{E}{B} + \left( v_{init} - \frac{E}{B} \right) \cos\left( \frac{\omega l}{v_{init}} \right)} \quad (47)$$

These equations were then used to construct the diagram of Figures 5, 6, and 7 based on a Matlab script for different values of magnetic field B and slit opening S given in percent of the total.



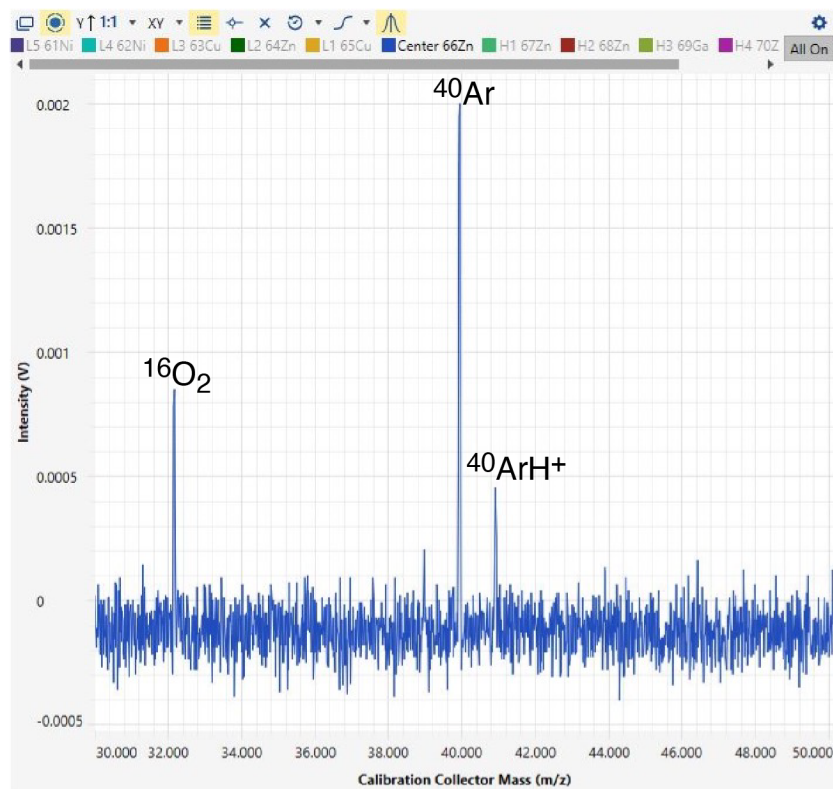


**Fig. S2:** Masses scan from 30 to 50 m/z with the axial mass set at  $^{66}\text{Zn}$  and  $B = 30\%$ ,  $E = 150$  V,  $S = 70\%$ .

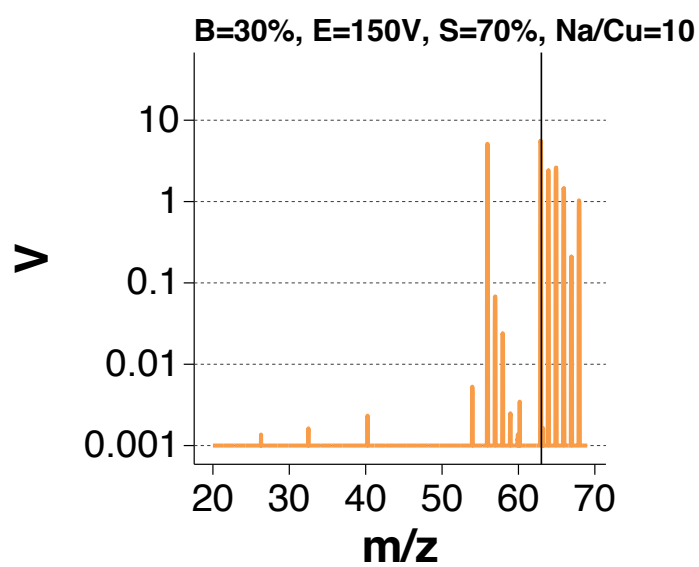


**Fig. S3:** Overall signal intensities for a mass scan from 20 to 70 m/z of a Cu-Zn-Na solution with Cu and Zn at 200 ng/ml and Na at 2  $\mu\text{g/ml}$ .

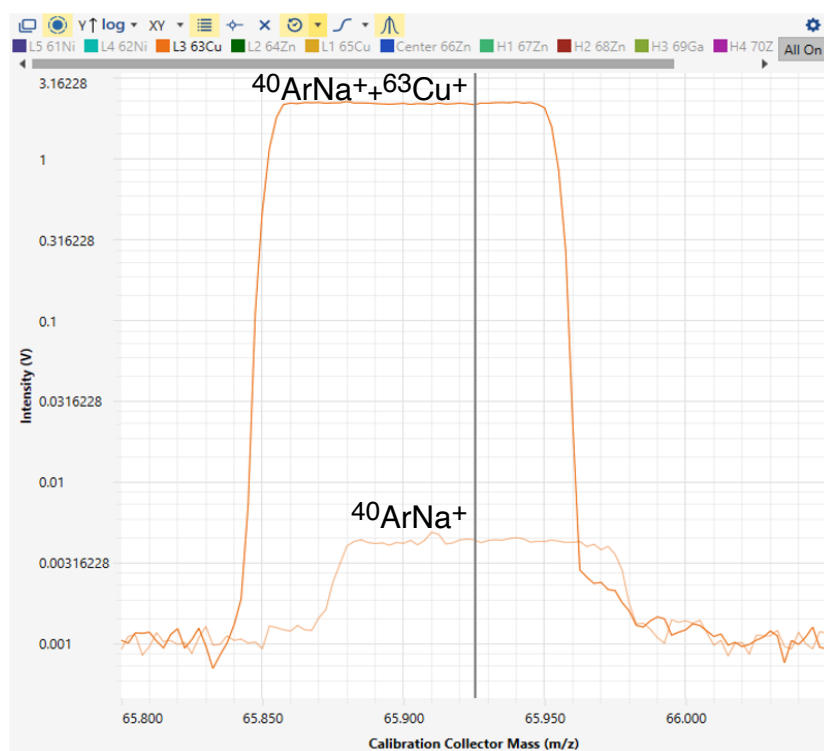


**Fig. S4:** Peak shapes with the axial mass set at  $^{66}\text{Zn}$  and  $B = 30\%$ ,  $E = 150 \text{ V}$ ,  $S = 70\%$  of a  $\text{HNO}_3$  0.05M + Na 2 ppm solution (light orange) and of Cu-Zn 200 ppb + Na 2 ppm solution (dark orange), showing the  $^{40}\text{ArNa}^+$  isobaric interference on  $^{63}\text{Cu}^+$ .

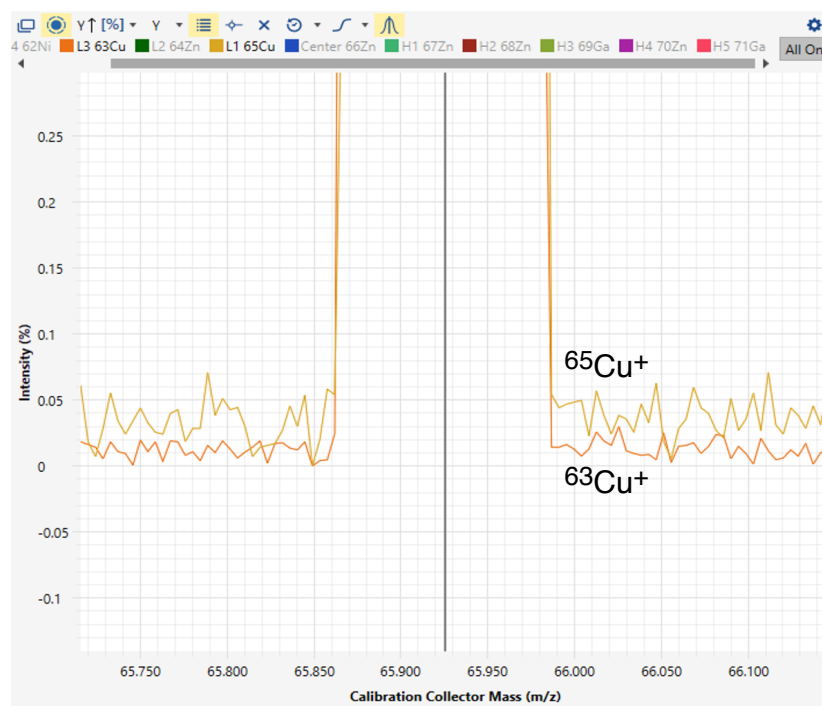


**Fig. S5:** Peak shapes with the axial mass set at  $^{66}\text{Zn}$  and  $B = 30\%$ ,  $E = 150\text{ V}$ ,  $S = 70\%$  of a Cu-Zn 200 ppb + Na 2 ppm solution with He as a collision gas set at 5 ml/min showing the complete removal of the  $^{40}\text{ArNa}^+$  isobaric interference on  $^{63}\text{Cu}^+$  (dark orange).

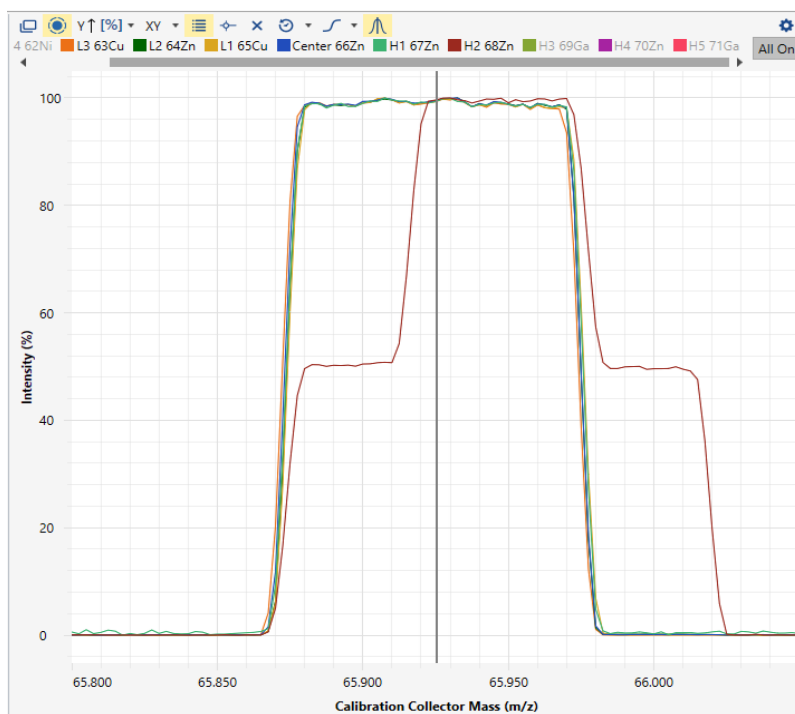


**Fig. S6:** Peak shapes with the axial mass set at  $^{66}\text{Zn}$  and  $B = 30\%$ ,  $E = 150\text{ V}$ ,  $S = 70\%$  of a Cu-Zn 200 ppb + Na 2 ppm solution with He as a collision gas set at 5 ml/min showing the isobaric interference on  $^{68}\text{Zn}^+$  (brown).

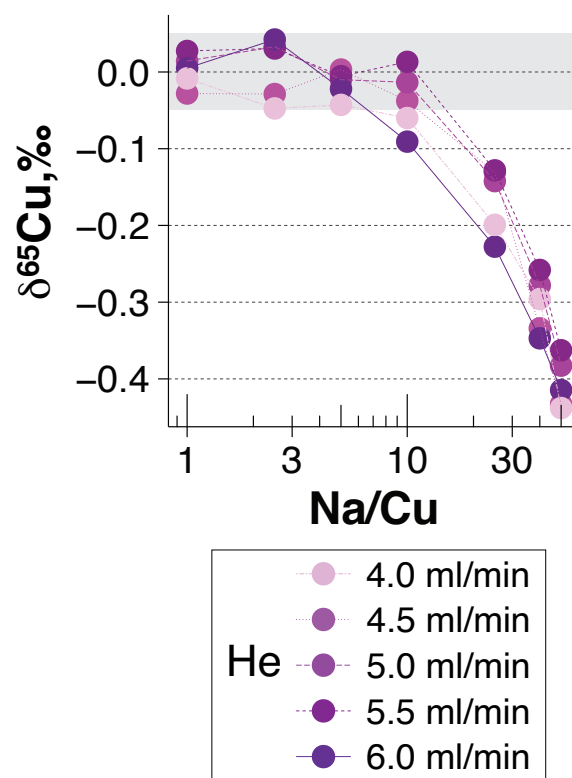


**Fig. S7:** Matrix effects on the  $\delta^{65}\text{Cu}$  value of the SRM-976 solution as a function of the Na/Cu ratio measured with the Neoma MS/MS. Several He flow are tested. The light grey area represents  $\pm 0.05\text{‰}$  deviation.

**Table S1:** Copper isotope compositions. § stands for Neoma MS/MS measurements and # stands for Nu Plasma measurements.

|                 | $\delta^{65}\text{Cu}$ , ‰ | $\pm 2\text{ SD}$ , ‰ | n    | Reference/Status            |                       |
|-----------------|----------------------------|-----------------------|------|-----------------------------|-----------------------|
| <b>Standard</b> |                            |                       |      |                             |                       |
| BHVO-1          | -0.05                      |                       | 1    | This study                  |                       |
|                 | -0.01                      | 0.08                  | 9    | Sullivan et al., 2020       |                       |
| JB1 a           | 0.06                       |                       | 1    | This study                  |                       |
| DNC 1           | 0.12                       |                       | 1    | This study                  |                       |
| W2a             | 0.11                       |                       | 1    | This study                  |                       |
|                 | 0.04                       | 0.09                  | 11   | Sullivan et al., 2020       |                       |
|                 | 0.10                       | 0.08                  | 4    | Liu et al., 2014            |                       |
|                 | 0.11                       | 0.05                  | 4    | Liu et al., 2014            |                       |
|                 | 0.11                       | 0.04                  | 4    | Liu et al., 2014            |                       |
|                 | BIR-1                      | 0.01                  |      | 1                           | This study            |
|                 |                            | -0.01                 | 0.08 | 9                           | Sullivan et al., 2020 |
| -0.02           |                            | 0.10                  | 31   | Li et al., 2009             |                       |
| 0.08            |                            | 0.07                  | 6    | Moeller et al., 2012        |                       |
| 0.00            |                            | 0.03                  | 2    | Sossi et al., 2015          |                       |
| 0.09            |                            | 0.08                  | 2    | Jeong et al., 2021          |                       |
| -0.02           |                            | 0.05                  | 4    | Liu et al., 2014            |                       |
| -0.01           |                            | 0.04                  | 6    | Liu et al., 2014            |                       |
| -0.03           |                            | 0.04                  | 4    | Liu et al., 2014            |                       |
| 0.01            |                            | 0.05                  | 4    | Liu et al., 2014            |                       |
| 0.02            |                            | 0.04                  | 4    | Liu et al., 2014            |                       |
| 0.02            |                            | 0.04                  | 3    | Liu et al., 2015            |                       |
| AGV-2           |                            | 0.09                  |      | 1                           | This study            |
|                 | 0.09                       | 0.02                  | 2    | Jeong et al., 2021          |                       |
|                 | 0.06                       | 0.04                  | 4    | Liu et al., 2014            |                       |
|                 | 0.05                       |                       | 1    | Liu et al., 2014            |                       |
|                 | 0.06                       |                       | 1    | Liu et al., 2015            |                       |
|                 | 0.10                       |                       | 1    | Weinstein et al., 2011      |                       |
|                 | -0.02                      | 0.06                  | 2    | Souto-Oliveira et al., 2019 |                       |
|                 | 0.10                       | 0.11                  | 8    | Moeller et al., 2012        |                       |
| RGM-1           | -0.01                      |                       | 1    | This study                  |                       |
| BCR-1           | 0.22                       |                       | 1    | This study                  |                       |
|                 | 0.07                       | 0.08                  | 6    | Archer and Vance, 2004      |                       |
|                 | 0.11                       | 0.12                  | 2    | Souto-Oliveira et al., 2019 |                       |
| <b>Sample</b>   |                            |                       |      |                             |                       |
| A2 - 33         | -0.71§                     |                       | 1    | Positive                    |                       |
|                 | -0.65#                     |                       | 1    |                             |                       |
| A3 - 61         | -0.19§                     |                       | 1    | Negative                    |                       |
|                 | -0.25#                     |                       | 1    |                             |                       |
| A5 - 56         | -0.09§                     |                       | 1    | Negative                    |                       |
|                 | -0.15#                     |                       | 1    |                             |                       |

## References

- C. Archer and D. Vance, *Journal of Analytical Atomic Spectrometry*, 2004, **19**, 656–665.
- H. Jeong, K. Ra and J. Y. Choi, *Geostandards and Geoanalytical Research*, 2021, **45**, 551–563.
- W. Li, S. E. Jackson, N. J. Pearson, O. Alard and B. W. Chappell, *Chemical Geology*, 2009, **258**, 38–49.
- S.-A. Liu, D. Li, S. Li, F.-Z. Teng, S. Ke, Y. He and Y. Lu, *J. Anal. At. Spectrom.*, 2013, **29**, 122–133.
- K. Moeller, R. Schoenberg, R.-B. Pedersen, D. Weiss and S. Dong, *Geostandards and Geoanalytical Research*, 2012, **36**, 177–199.
- P. A. Sossi, G. P. Halverson, O. Nebel and S. M. Eggins, *Geostandards and Geoanalytical Research*, 2015, **39**, 129–149.
- C. E. Souto-Oliveira, M. Babinski, D. F. Araújo, D. J. Weiss and I. R. Ruiz, *Atmospheric Environment*, 2019, **198**, 427–437.
- K. Sullivan, D. Layton-Matthews, M. Leybourne, J. Kidder, Z. Mester and L. Yang, *Geostandards and Geoanalytical Research*, 2020, **44**, 349–362.
- C. Weinstein, F. Moynier, K. Wang, R. Paniello, J. Foriel, J. Catalano and S. Pichat, *Chemical Geology*, 2011, **286**, 266–271.